J. Micromech. Microeng. **9** (1999) 230–235. Printed in the UK PII: S0960-1317(99)98357-2

Determination of the elastic modulus of thin film materials using self-deformed micromachined cantilevers

Weileun Fang

Power Mechanical Engineering Department, National Tsing Hwa University, Hsinchu, Taiwan

Received 13 October 1998

Abstract. The elastic modulus is a very important mechanical property in micromachined structures. There are several design issues such as resonant frequencies and stiffness in micromachined structures that are related to the elastic modulus. In addition, the accuracy of the results from a finite element model is highly dependent upon the elastic modulus. In this study a simple technique to characterize the elastic moduli of thin films of any thickness was developed. The film to be measured formed a bilayer cantilever with another film through standard micromachining processes. Due to the residual stresses of these two films the bilayer cantilever was deformed without any external load. Through the deformation profile of this self-deformed bilayer cantilever, the elastic modulus of the deposited film was determined. A theoretical model was developed to predict the variations of the elastic modulus of a deposited film and the deformation profile of a bilayer cantilever. Experiments were also conducted to demonstrate the applications of this approach. In the experiments, bilayer cantilevers constructed from thin films of different materials and residual stresses were fabricated and measured.

1. Introduction

Thin film materials are used widely in the areas of microelectronics, magnetic recording systems, microelectromechanical systems, etc [1, 2]. The thickness of the thin film materials can range from several hundred angstrom, for example the overcoat of a hard disk, to several microns, for example a micromotor. In order to improve the performance of thin film devices, it is necessary to characterize their mechanical as well as electrical properties. The elastic modulus is a very important mechanical property. There are several design issues related to the elastic modulus such as resonant frequencies and stiffness. In addition, the accuracy of the results from finite element analysis is also very dependent on the elastic modulus.

Because thin films have thicknesses of the order of microns, the traditional elastic modulus determination techniques used for bulk materials, such as the tensile test, are not applied extensively [3]. In addition, the test in [3] requires a special experimental setup and specimen. On the other hand, the elastic moduli for components on the dimensional scale of microns are not evident in advance, and particularly so, to the extent that the process by which the thin film is grown affects the material properties [4, 5]. For instance, the ion bombardment effect may change the residual stress and elastic modulus of a sputtered film [4]. The elastic modulus of a thermal oxide depends upon the growing process (wet or dry) [5]. Therefore, it is not reliable to predict thin film material properties from bulk material or through extrapolations of thick film properties.

Currently several techniques in addition to [3] have been developed to characterize the elastic moduli of thin film materials. For example, the load–deflection tests on microstructures through the load from electrostatic voltage and pressure have been discussed [6, 7]. Unfortunately a complicated experimental setup is required for these measurement techniques. The load–deflection tests using a surface profiler [8] and nanoindenter [9] are also available. In these two approaches, mechanical contact between the probe and the micromachined structures during the measurement is inevitable. This may lead to some unwanted effects such as friction during the measurement. Indirect methods devised for determining the elastic moduli of thin films include techniques that involve measurement of the resonant frequencies of micromachined beams [10–12]. An additional experimental setup is also required to excite the micromachined structures for measuring their resonant frequencies.

This study intends to develop a simple technique to characterize the elastic moduli of thin films of any thickness. In this technique, the film to be measured will be deposited on top of a film with known material properties. As shown

0960-1317/99/030230+06$30.00

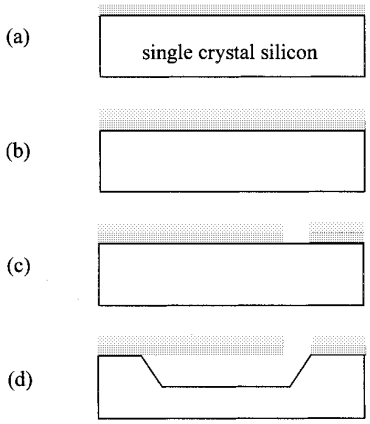

Figure 1. Fabrication processes of the bilayer cantilever: (a) single-crystal silicon and a film with known material property; (b) deposition of the film to be measured; (c) patterning; (d) anisotropic etching.

in figure 1, these two films form a bilayer cantilever after a standard bulk micromachining process. Due to the mismatch of the residual strains for these two films, the bilayer cantilever will be deformed without any external loading. Through the deformation profile of this self-deformed bilayer cantilever, the elastic modulus of the deposited film is determined. In the following text, a theoretical model is developed to predict the relationship between the elastic modulus of a deposited film and the deformation profile of a bilayer cantilever. Experiments are also conducted to demonstrate the applications of the proposed technique. Thus, the elastic moduli of the thin films are determined after the diagnostic micromachined cantilevers are fabricated and measured.

2. Theoretical analysis

Thin film materials, which were grown or deposited on top of a substrate, have normally existing residual stresses. For the first approximation, the residual stresses can be represented using [13]

$$\sigma_{total} \approx \sigma_0 + \sigma_1 \left(\frac{y}{h/2} \right). \tag{1}$$

In (1), σ_0 represents a uniform residual stress (either in compression or in tension) and σ_1 represents a gradient residual stress. The uniform residual stress σ_0 of the thin film will be relieved through the free end of a single-layer cantilever. On the other hand, the single-layer cantilever will be bent by the gradient residual stress σ_1 with a radius of curvature

$$\rho = \frac{Eh}{2\sigma_1} \tag{2}$$

where $E = E_f/(1 - \nu_f)$ is the biaxial elastic modulus and E_f and ν_f are the elastic modulus and Poisson's ratio respectively of the thin film. The model problem considered here as illustrated in figures 2 and 3 corresponds to a micromachined cantilever that consists of two different films as shown in figure 1(d). This situation arises, for instance, when a plasma enhanced chemical vapour deposition (PECVD) nitride film is deposited onto a thermal

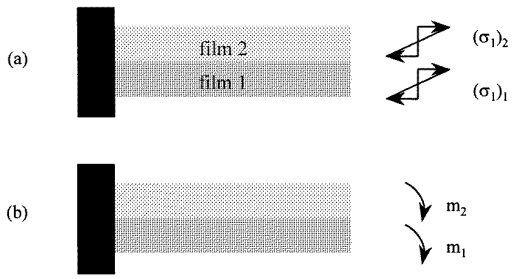

Figure 2. (a) A bilayer cantilever under gradient residual stresses $(\sigma_1)_i$ and (b) the loadings applied on the bilayer cantilever after the release of the gradient residual stresses.

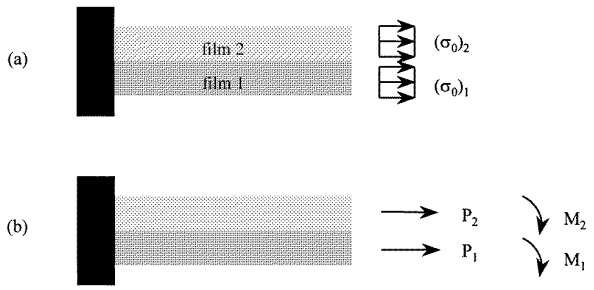

Figure 3. (a) A bilayer cantilever under uniform residual stresses $(\sigma_0)_i$ and (b) the loadings applied on the bilayer cantilever after the release of the uniform residual stresses.

oxide film and then patterned and etched into a cantilever. Due to the relief of the residual stresses the bilayer cantilever will be deformed, although there are no external forces or moments. This self-deformed bilayer cantilever is exploited in this research to determine the elastic moduli of the thin films.

The uniform residual stresses and gradient residual stresses for the films of the bilayer cantilever illustrated in figures 2(a) and figure 3(a) are $(\sigma_0)_i$ and $(\sigma_1)_i$ (i is the index for different films, $i = 1$ to 2) respectively. The bilayer cantilever will be bent after the gradient residual stresses as well as the uniform residual stresses are relieved from the films. Hence, the net deflection of the bilayer cantilever will be superposed by the deflections lead by both $(\sigma_0)_i$ and $(\sigma_1)_i$. In short, the proposed analytical model is more accurate than the conventional bimetallic cantilever model [14] by introducing the effect of the gradient residual stress $(\sigma_1)_i$. After the gradient residual stresses are relieved from the films, there is a resultant bending moment m_i acting over the etched films as shown in figure 2(b). The moment m_i corresponding to the biaxial elastic modulus E_i $(=E_{fi}/(1 - \nu_{fi}))$, the moment of inertia I_i, and the radius of curvature ρ_i for each film is simply $m_i = E_i I_i/\rho_i$. Thus, the bilayer beam is bent with a radius of curvature $\rho_{gradient}$ by the total bending moment $\sum m_i$ [15]

$$\rho_{gradient} = \frac{E_1 I_{effective}}{m_1 + m_2} = \frac{12 I_{effective}}{\frac{h_1^3}{\rho_1} + \frac{e_1 h_2^3}{\rho_2}} \tag{3}$$

where h_i is the thickness of the films and $e_1 = E_2/E_1$. In (3), ρ_1 and ρ_2 are the radii of curvature of the single-layer cantilevers made from films 1 and 2, respectively. In addition, $I_{effective}$ is the effective moment of inertia of the

bilayer cantilever [15],

$$I_{effective} = \frac{e_1 h_2^3}{12} + e_1 h_2 \left(h_1 + \frac{h_2}{2} - \bar{y} \right)^2 + \frac{h_1^3}{12} + h_1 \left(\frac{h_1}{2} - \bar{y} \right)^2$$

$$\bar{y} = \frac{e_1 h_2 \, (h_1 + h_2/2) + h_1^2/2}{e_1 h_2 + h_1}. \quad (4)$$

If the thickness of the film to be measured is very small (i.e. $h_2 \ll h_1$), it is obtained from (3) and (4) that $\rho_{gradient} \approx \rho_1$.

The uniform residual stress can be relieved through the free end for a single-layer cantilever. However, for a bilayer cantilever, it will be exposed to a bending moment by the uniform residual stresses if the uniform residual strains $(\epsilon_0)_1$ and $(\epsilon_0)_2$ of the thin films are different. After the uniform residual stresses are relieved from the films, there are resultant normal forces P_i and moments M_i acting over each film as shown in figure 3(b). Since no external forces and moments are applied to the films, the basic requirement for this bilayer cantilever is to satisfy $\sum P = 0$ and $\sum M = 0$. It is evident for this self-deformed structure that

$$P_1 + P_2 = 0 \qquad M_1 + M_2 = P_1 \frac{h_1}{2} + P_2 \left(h_1 + \frac{h_2}{2} \right) \quad (5)$$

hence $P_1 = -P_2$ and $M_1 + M_2 = P_2(h_1 + h_2)/2$. In order to satisfy the equation of compatibility, the total strain for films 1 and 2 must be equal at their interface. Since the cantilever is bent with a radius of curvature $\rho_{uniform}$, the compatibility equation becomes

$$-\frac{(\sigma_0)_2}{E_2} + \frac{P_2}{E_2 h_2 w} + \frac{h_2}{2\rho_{uniform}} = -\frac{(\sigma_0)_1}{E_1} + \frac{P_1}{E_1 h_1 w} - \frac{h_1}{2\rho_{uniform}} \quad (6)$$

where w is the width of the films. Note that there are negative signs for both $(\sigma_0)_1$ and $(\sigma_0)_2$, since they are residual stresses. The radius of curvature $\rho_{uniform}$ determined through (5) and (6) is

$$\rho_{uniform} = \left(\frac{-\frac{1/e_1 + H_1^3}{6(H_1 + H_1^2)} - \frac{1 + e_1 H_1^3}{6(1 + H_1)} - \frac{H_1}{2} - \frac{1}{2}}{(\sigma_0)_1 - \frac{(\sigma_0)_2}{e_1}} \right) E_1 h_1 \quad (7)$$

where $H_1 = h_2/h_1$ is a non-dimensional parameter. Therefore, the net radius of curvature of the bent bilayer beam ρ_{total} is

$$\frac{1}{\rho_{total}} = \frac{1}{\rho_{gradient}} + \frac{1}{\rho_{uniform}}. \quad (8)$$

Substitution of (3), (4) and (7) into (8) results in the following relationship

$$E_2 = f(\rho_{total}, h_1, h_2, \rho_1, \rho_2, (\sigma_0)_1, (\sigma_0)_2, E_1). \quad (9)$$

Therefore, the biaxial elastic modulus E_2 can be determined through (9).

3. Applications and results

In applications of this technique, a PECVD nitride film has been used in the case studies. Bilayer cantilevers with a length between 40 and 200 μm were fabricated through conventional bulk micromachining in this experiment. Cantilevers of different lengths were used to check the uniformity of the fabrication and the repeatability and consistency of the measurements. Since the material properties of the thermally grown SiO_2 have been extensively studied [5, 16, 17], it was chosen as the base layer of the bilayer cantilever. In short, the bilayer cantilevers consisted of thermal SiO_2 and PECVD nitride. As shown in figures 1(a) and (b), the SiO_2 film was thermally grown onto a (100) wafer at 1050 °C first and then deposited with a nitride film. Both of these two films were patterned using lithography and buffered hydrofluoric acid as illustrated in figure 1(c). The bilayer cantilevers were suspended above a cavity as shown in figure 1(d), after the substrate was etched anisotropically with N_2H_4. Since the selectivity between single crystal silicon and the thin films is very large for N_2H_4, the removal of the thin films during the etching process is negligible. The SEM photograph in figure 4 shows several typical micromachined cantilevers.

The deformation configuration of the micromachined cantilevers was measured quantitatively using an interferrometric profilometry. A typical deflection profile of a bilayer micromachined cantilever measured in this manner is shown in figure 5. Hence the radius of curvature of the bilayer cantilever ρ_{total} is determined from the measured profiles. The radius of curvature of SiO_2 and PECVD nitride single-layer cantilevers ρ_1 and ρ_2 were also characterized in the same manner. In addition, the residual stresses $(\sigma_0)_1$ and $(\sigma_0)_2$ of the films was characterized using a commercialized thin film stress measurement instrument in this experiment. The residual stresses were determined by measuring the change in the global curvature of a wafer after the deposition of the thin film [18]. In the experiment, the residual stress $(\sigma_0)_1$ of film 1 is considered to be unchanged after the deposition of film 2. With E_1, h_1 and h_2 being determined from the measured biaxial elastic moduli and thicknesses, E_2 was found in turn through equation (9).

In the case study, the SiO_2 film was 0.33 μm thick and the PECVD nitride film was 0.30 μm thick. Figure 6(a) and (b) shows the measured configuration of SiO_2 and PECVD nitride single-layer cantilevers, respectively. According to the measurements, the average radius of curvature for SiO_2 and PECVD nitride cantilevers were $\rho_1 = 360$ μm and $\rho_2 = 780$ μm, respectively. In addition, the radius of curvature of the bilayer cantilever determined using the profile in figure 5 was $\rho_{total} = -190$ μm. The residual stresses of the SiO_2 and PECVD nitride films characterized through the wafer curvature approach were $(\sigma_0)_1 = -290$ MPa and $(\sigma_0)_2 = -1120$ MPa, respectively. Since the elastic modulus and the Poisson's ratio of the wet thermal SiO_2 is 70 GPa and 0.15, respectively, the biaxial elastic modulus of film 1 is $E_1 = 82$ GPa. Therefore, the relationship between E_2 and ρ_{total}, shown in figure 7, is determined through (9).

As indicated in figure 7, the bilayer cantilever is initially bent downward with $\rho_{total} = -6$ μm at $E_2 = 10$ GPa. The radius of curvature of the bilayer cantilever is changed to -2000 μm when E_2 is increased to 275 GPa. When E_2 is near 300 GPa, ρ_{total} becomes very large; in other words, the bilayer cantilever is flat. After E_2 is greater than 310 GPa, the bilayer cantilever is bent upward, and the radius

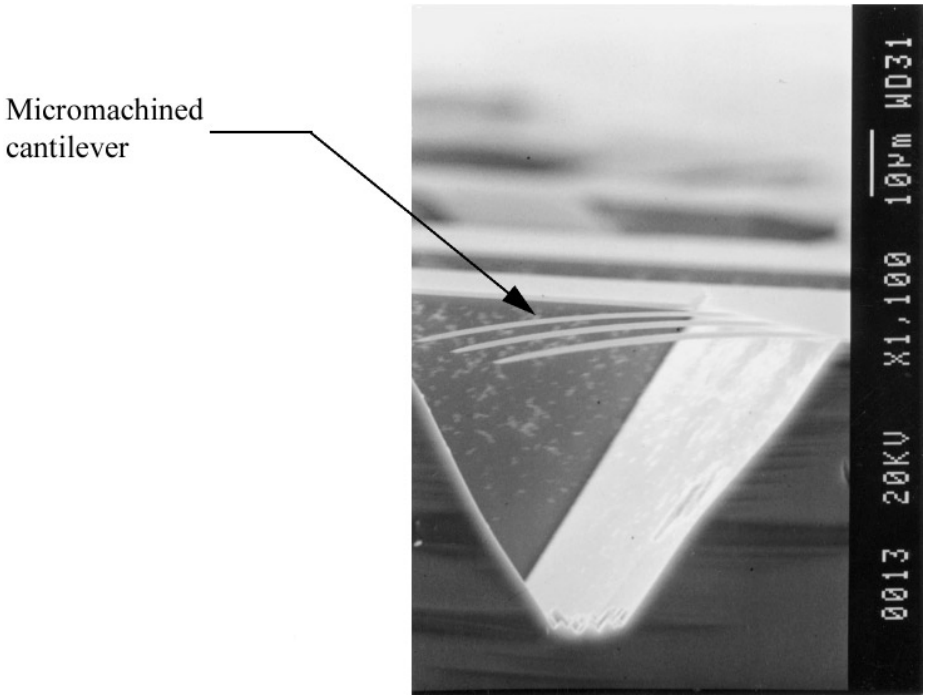

Figure 4. SEM photograph of the bilayer cantilevers.

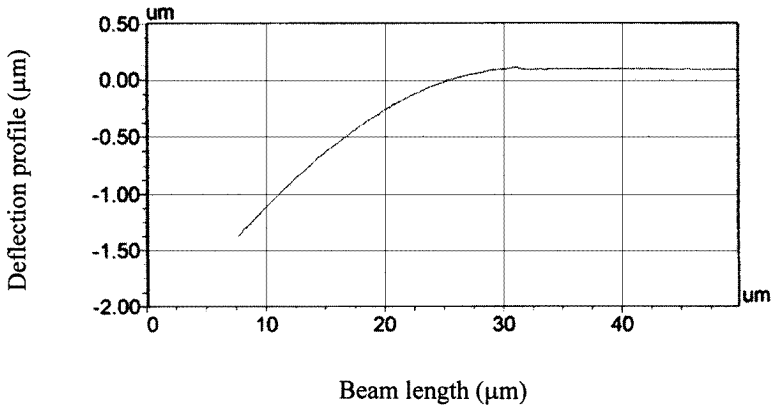

Figure 5. The measured deformation configuration of a 25 μm long bilayer beam from interferometric profilometry.

of curvature of the bilayer cantilever is decreased when E_2 is increased. The configurations of the bilayer cantilever for different E_2 are also depicted by the insets in figure 7. Since $\rho_{total} = -190\ \mu$m, the biaxial elastic modulus of the PECVD nitride film in this experiment is $E_2 = 182$ GPa. Thus the elastic modulus of the PECVD nitride film is $E_{f2} = 137$ GPa for the Poisson's ratio of PECVD nitride film $\nu_{f2} = 0.25$ [19]. By way of comparison with the existing results, the biaxial elastic modulus of the PECVD nitride film is distributed from 85 GPa to 210 GPa [19].

4. Discussion

In general, micromachined structures are always deformed by the thin film residual stresses. The proposed technique exploits this characteristic to determine the elastic moduli of thin films. The advantages of such an approach are twofold: first, the structure is self-deformed, hence no complicated setup for applying external loads is required; and second, the error due to the initial deflection during measurement, such as the deviation of the resonant frequencies, can be prevented. Furthermore, it is recommended to characterize the thin film material properties through multiple approaches in order to reach a reliable result. Thus, the existing techniques [5–12], in which the elastic modulus is determined by complicated setups, can be supplemented with the use of the bilayer cantilever technique.

The results according to the simulations of thin films with $h_2 = 0.1\ \mu$m and $0.3\ \mu$m thick Si_3N_4 film deposited onto a $h_1 = 1\ \mu$m thick SiO_2 base layer is shown in figure 8. The three different curves in figure 8 represent the variations of E_2 and ρ_{total} for radii of curvature $\rho_2 = 780\ \mu$m, $7800\ \mu$m and $-780\ \mu$m, respectively. In comparisons with the results shown in figures 8(a) and (b), it is evident that the relationship between ρ_{total} and E_2 will not be influenced by ρ_2 for smaller h_2. Thus, it is not necessary to characterize the radius of

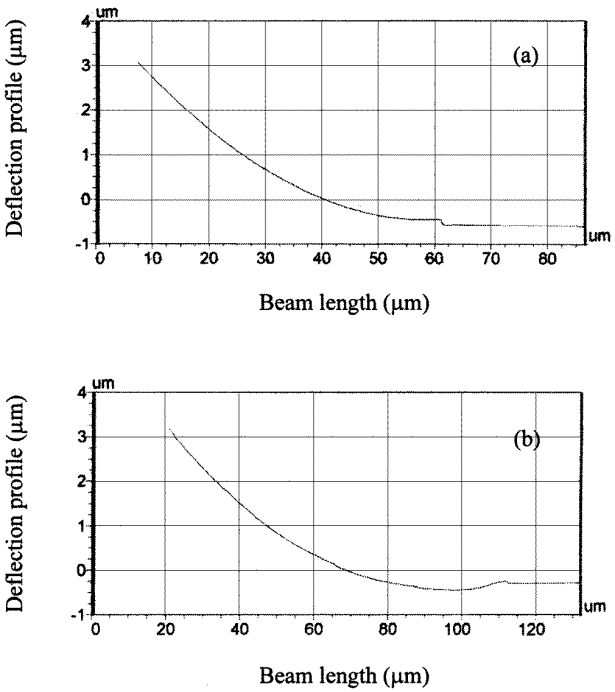

Figure 6. The measured deformation configuration of: (a) a SiO_2 cantilever; and (b) a PECVD nitride cantilever.

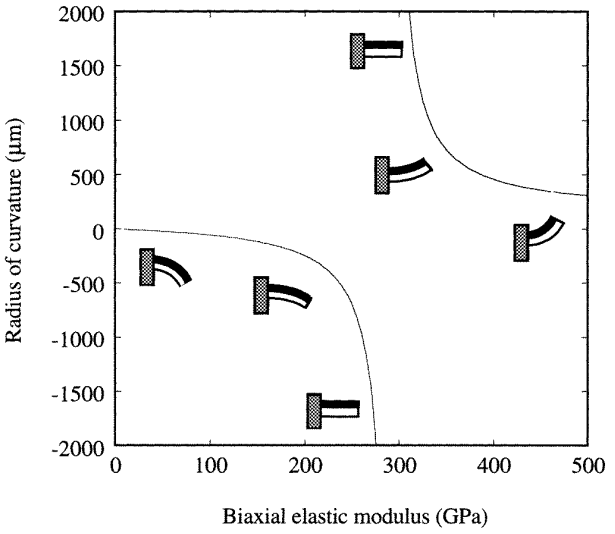

Figure 7. The variation of the biaxial elastic modulus E_2 and the radius of curvature of the bilayer beam ρ_{total}.

curvature ρ_2 when the thickness of the film h_2 is very thin. The difficulty in determining the gradient residual stress of film 2 when h_2 is very thin can be prevented.

The residual stresses $(\sigma_0)_1$ and $(\sigma_0)_2$ of the thin films were determined through the variations of the wafer curvature in this study. This approach only gives an average measure of the stress across the entire substrate. In addition, the irregular surface topology of the substrate may lead to an error in stress measurement. Therefore errors of the biaxial elastic modulus E_2 determined through (9) are produced by the error of the measured residual stress $(\sigma_0)_2$. For instance,

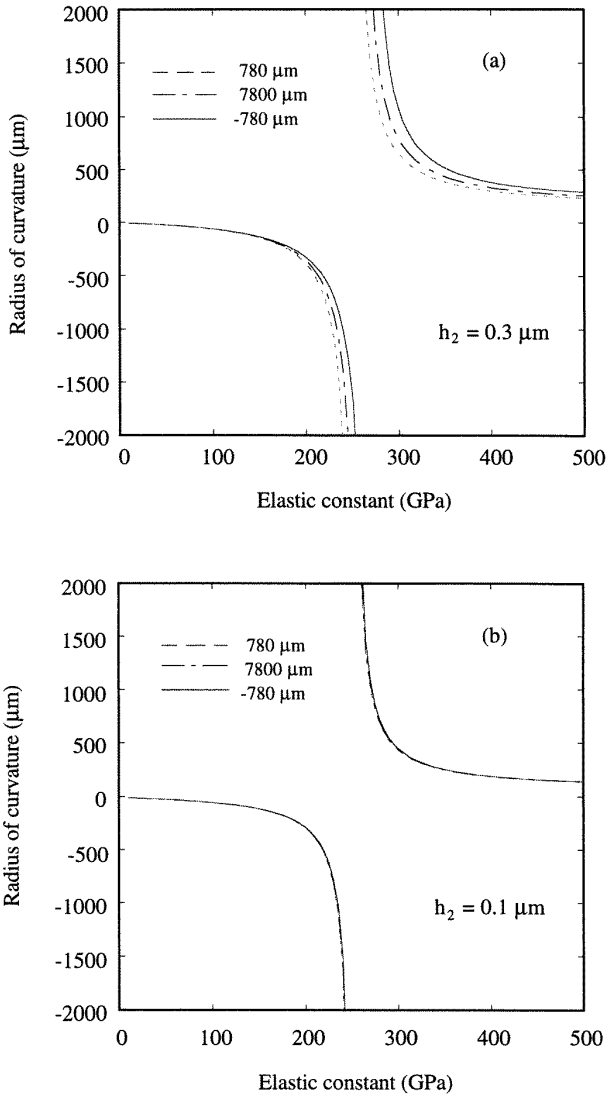

Figure 8. The variation of E_2 and ρ_{total} for three different radii of curvature ρ_2 when the film thickness h_2 is: (a) 0.3 μm; and (b) 0.1 μm.

the error propagation between $(\sigma_0)_2$ and E_2 is

$$\frac{\mathrm{d}E_2}{E_2} = \left(-\frac{E_1 h_1}{6\rho_{total}(\sigma_0)_2(H_1 + H_1^2)} + \frac{E_1 h_1 e_1^2 H_1^3}{6\rho_{total}(\sigma_0)_2(1 + H_1)} + 1 \right)^{-1} \frac{\mathrm{d}(\sigma_0)_2}{(\sigma_0)_2}. \quad (10)$$

It is obvious from (10) that a limiting case of the error propagation is $\mathrm{d}E_2/E_2 \approx \mathrm{d}(\sigma_0)_2/(\sigma_0)_2$. In order to prevent the error of the elastic modulus due to the measurement of $(\sigma_0)_1$ and $(\sigma_0)_2$ of the thin films, (7) can be rewritten as

$$\rho_{uniform} = \left(\frac{-\frac{1/e_1+H_1^3}{6(H_1+H_1^2)} - \frac{1+e_1 H_1^3}{6(1+H_1)} - \frac{H_1}{2} - \frac{1}{2}}{(\varepsilon_0)_1 - (\varepsilon_0)_2} \right) h_1. \quad (11)$$

In (11), the residual strains $(\varepsilon_0)_1$ and $(\varepsilon_0)_2$ of the thin films is used to replace the residual stresses of the thin films. Since the residual strains can be determined through diagnostic micromachined beams [13], a more accurate measured value

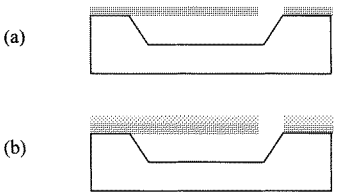

Figure 9. Fabrication processes of the bilayer cantilever through: (a) the fabrication of a single-layer cantilever; and (b) the deposition of a second thin film.

can be obtained. Moreover, the distribution of the residual strain can also be measured through the same approach. However, this approach cannot be applied for a very thin film.

In the presented case, the thin films of the bilayer cantilever were patterned first and then undercut simultaneously as shown in figures 1(c) and 1(d). This is different from the case discussed in [20], where film 2 was deposited after the cantilevers made from film 1 were fabricated as shown in figure 9. Therefore the uniform residual stress of film 1 has no contribution to the bending of the bilayer cantilever in [20]. In other words, (9) is not appropriate for determining the biaxial elastic moduli of thin films fabricated through the processes illustrated in figure 9.

Acknowledgments

This material is based (in part) upon work supported by the National Science Council (Taiwan) under Grant NSC 87-2218-E007-007. The author would also like to express his appreciation for the assistance of his graduate students Jerwei Hsieh, Hung-Yi Lin and Hsing-Hua Hu of National Tsing Hua University (Taiwan) in handling the fabrication processes.

References

[1] Petersen K E 1982 Silicon as a mechanical material *Proc. IEEE* **70** 420–57
[2] Nix W D 1991 Mechanical properties of thin films *Metall. Trans.* A **20** 2217–45
[3] Sharpe W N Jr, Yuan B and Edwards R L 1997 A new technique for measuring the mechanical properties of thin films *J. Microelectromech. Syst.* **6** 193–9
[4] Thornton J A and Hoffman D W 1989 Stress-related effects in thin film *Thin Solid Films* **171** 5–31
[5] Petersen K E and Guarnieri C R 1979 Young's modulus measurements of thin films using micromechanics *J. Appl. Phys.* **50** 6761–5
[6] Najafi K and Suzuki K 1989 A novel technique and structure for the measurement of intrinsic stress and Young's modulus of thin films *Proc. IEEE/MEMS (Salt Lake City, UT, February 1989)* pp 96–7
[7] Tabata O, Kawahata K, Sugiyama S and Igarashi I 1989 Mechanical property measurements of thin films using load–deflection of composite rectangular membrane *Sensors Actuators* A **20** 135–41
[8] Tai Y-C and Muller R S 1990 Measurement of Young's modulus on microfabricated structures using a surface profiler *Proc. IEEE/MEMS (Napa Valley, CA, February 1990)* pp 11–14
[9] Doerner M F and Nix W D 1986 A method for interpreting the data from depth-sensing indentation instruments *J. Mater. Res.* **1** 601–9
[10] Kiesewetter L, Zhang J-M, Houdeau D and Steckenborn A 1992 Determination of Young's moduli of micromechanical thin films using the resonance method *Sensors Actuators* A **35** 153–9
[11] Zhang L M, Uttamchandani D and Culshaw B 1991 Measurement of the mechanical properties of silicon microresonators *Sensors Actuators* A, **29** 79–84
[12] Zhang L M, Uttamchandani D, Culshaw B and Dobson P 1990 Measurement of Young's modulus and internal stress in silicon microresonators using a resonant frequency technique *Meas. Sci. Technol.* **1** 1343–6
[13] Fang W and Wickert J A 1996 Determining mean and gradient residual stresses in thin films using micromachined cantilevers *J. Micromech. Microeng.* **6** 301–9
[14] Chu W-H, Mehregany M and Mullen R L 1993 Analysis of tip deflection and force of a bimetallic cantilever microactuator *J. Micromech. Microeng.* **3** 4–7
[15] Beer F P and Johnston E R Jr 1981 *Mechanics of Materials* (New York: McGraw-Hill)
[16] Jaccodine R J and Schlegel W A 1966 Measurement of strains at Si–SiO_2 interface *J. Appl. Phys.* **37** 2429–34
[17] Wolf S and Tauber R N 1986 *Silicon Processing* (Sunset Beach, CA: Lattice)
[18] Rossnagel S M, Gilstrap P and Rujkorakarn R 1982 Stress measurement in thin films by geometrical optics *J. Vac. Sci. Technol.* B **21** 1045–6
[19] Stoffel A, Kovacs A, Kronast W and Muller B 1996 LPCVD against PECVD for micromechanical applications *J. Micromech. Microeng.* **6** 1–13
[20] Fang W and Wickert J A 1995 Comments on measuring thin-film stresses using bi-layer micromachined beams *J. Micromech. Microeng.* **5** 276–81